Computational Materials Science 159 (2019) 316–326

Contents lists available at ScienceDirect

Computational Materials Science

journal homepage: www.elsevier.com/locate/commatsci

Nonequilibrium free-energy calculations of fluids using LAMMPS

Rodolfo Paula Leite[a,*], Maurice de Koning[a,b]

[a] Instituto de Física "Gleb Wataghin", Universidade Estadual de Campinas, UNICAMP, 13083-859 Campinas, São Paulo, Brazil
[b] Center for Computational Engineering & Sciences, Universidade Estadual de Campinas, UNICAMP, 13083-861 Campinas, São Paulo, Brazil

ARTICLE INFO

Keywords:
Nonequilibrium free-energy calculations
Molecular dynamics
Fluids
LAMMPS

ABSTRACT

We present a guide to compute the absolute free energies of classical fluids using nonequilibrium free-energy techniques within the LAMMPS (Large-scale Atomic/Molecular Massively Parallel Simulator) code. The main approach is based on the construction of a thermodynamic path connecting the fluid of interest to either atomic or molecular variants of the Uhlenbeck-Ford (UF) model as reference systems. We describe these reference systems in detail, discuss their implementation in the LAMMPS package and make available source code, scripts as well as auxiliary files. As an illustration we detail a number of distinct applications, involving systems characterized by fundamentally different interactions. In addition to two different atomic models (mW water and the MEAM-2NN CuZr liquid binary alloy), we consider three molecular models for water, two of them rigid (TIP4P and SPC/E) and one flexible (q-SPC/Fw). For the molecular models we develop UF-based reference systems for which the free energies are given by a sum of two contributions: an intermolecular part described by the known UF free energy and an intramolecular contribution that can be determined analytically. The tools described in this paper provide a platform on which fluid-phase free energies can be easily and efficiently computed using the LAMMPS code. In addition to being useful for the development of new models for liquid phases, the tools may also find applications in the construction of community databases containing thermodynamic properties of existing models.

1. Introduction

Free energies are among the most important quantities in the description of condensed-phase systems and atomistic simulation techniques are very frequently used for their calculation. Nonetheless, neither free energies nor entropies can be expressed in terms of ensemble averages and therefore cannot be determined directly from simulations. By virtue of this difficulty, countless indirect methods to compute free energies have been developed [1]. One of the most applied approaches is the Hamiltonian interpolation (HI) method (also referred to as thermodynamic integration (TI) and λ-integration), [2–5] which computes the free-energy difference between the system of interest and a reference, for which the free energy is known, by constructing a sequence of equilibrium states along a thermodynamic path between them. Specifically, the free-energy difference is determined by computing ensemble averages of the thermodynamic driving force for a number of states on this path through a set of independent equilibrium simulations, followed by numerical integration. In recent years, nonequilibrium (NE) versions of the HI approach have become popular [6–8], in particular due to the rigorous connection between NE processes and equilibrium free-energy differences as encoded in Jarzynski's equality [9–11]. Contrary to equilibrium HI methods, NE approaches estimate the desired free-energy difference by traversing the thermodynamic path between the system of interest and the reference in an explicitly time-dependent process and have shown to give accurate results using only a few relatively short non-equilibrium simulations.

For the particular case of solids, either crystalline or amorphous, the choice of reference system is straightforward, with the Einstein crystal [12–14] providing a system with analytically known free energy. For fluid-phase systems, on the other hand, the choice is less obvious. At first sight, the ideal gas seems a natural pick as a reference since its free energy is known analytically. However, a direct switching path connecting an interacting fluid of interest to the ideal gas may cross a liquid-vapor coexistence line, hampering reversibility due to the presence of appreciable hysteresis [15]. Several strategies have been devised to avoid these difficulties. One of these is to divide the switching process into two stages [16,17], first introducing an intermediate, purely repulsive reference system, followed by a second stage transforming the repulsive model into the ideal gas. Another frequently adopted approach is to use an interacting fluid with a known free energy as a reference. One example is the Lennard-Jones (LJ) fluid [18,19], for which extensive numerical data is available [20].

* Corresponding author.
E-mail address: pl.rodolfo@gmail.com (R. Paula Leite).

https://doi.org/10.1016/j.commatsci.2018.12.029
Received 15 August 2018; Received in revised form 13 December 2018; Accepted 14 December 2018
Available online 21 December 2018
0927-0256/

Recently, we discussed the Uhlenbeck-Ford (UF) model and its generalizations as an alternative interacting reference system for fluid-phase free-energy calculations [21–23]. They are characterized by ultrasoft, purely repulsive pairwise interactions for which the Helmholtz free energies are fully characterized by functions of a single adimensional density variable and temperature appears only as a scaling factor. Moreover, the interactions decay as quickly and smoothly as a Gaussian, dispensing the need for choosing a particular truncation and/or shifting scheme with accompanying long-range corrections, as usually required for the LJ system [24].

Here we discuss the application of the UF-based reference system in the calculation of fluid-phase free energies, focusing on the implementation in the widely used `LAMMPS` molecular dynamics (MD) package [25]. We show how, together with NE free-energy techniques, the UF models can be used to accurately and efficiently compute free energies of both atomic as well as molecular liquids. We provide excerpts from the used `LAMMPS` scripts to exemplify the practical details of the calculations. Complete `LAMMPS` scripts, source codes and post-processing tools are also made available. In this sense, the present paper is similar to Ref. [8] in which the calculation of solid-phase free energies using LAMMPS were discussed in detail. As illustrations we perform free-energy computations for two atomic liquids and three molecular models for water. Specifically, for the former we consider the coarse-grained atomic water (mW) model [26] and a Cu-Zr liquid alloy described in terms of an MEAM-2NN potential [27–31]. The molecular water systems concern the rigid TIP4P [32] and SPC/E [33] potentials as well as the flexible q-SPC/Fw model [34]. For these water models we construct rigid and flexible interacting molecular reference systems based on the UF models such that their free energies are given by a sum of two contributions: an intermolecular part described by the known UF free energy and an intramolecular contribution that can be determined analytically.

The remainder of the paper is organized as follows. In Section 2 we provide a brief review of the NE methods used to compute free-energy differences between two equilibrium states. In Section 3, we describe in detail the UF-based reference systems for atomic and water-like molecular fluids. Next, in Section 4, we illustrate the implementation and application of these methods within the `LAMMPS` code, reporting the results for the above-mentioned systems and providing script excerpts. Finally, we end with a summary in Section 5.

2. Nonequilibrium free-energy methods

One of the widely-used methods to estimate free energy differences is the equilibrium TI technique introduced by Kirkwood in 1935 [2]. It consists of the construction of a path connecting two generic well-defined thermodynamic states by defining a parametrized Hamiltonian $H(\lambda)$, where λ is a coupling parameter describing the interpolation between the two ends of the thermodynamic path.

According to the second law of thermodynamics, the reversible work $W_{\rm rev}$ done along such a Hamiltonian-interpolation (HI) path is equal to the free-energy difference between the two equilibrium systems corresponding to $H(\lambda_i)$ and $H(\lambda_f)$, i.e.

$$\Delta F \equiv F(\lambda_f) - F(\lambda_i) = W_{\rm rev} = \int_{\lambda_i}^{\lambda_f} \left\langle \frac{\partial H}{\partial \lambda} \right\rangle_\lambda d\lambda, \tag{1}$$

where $\langle \cdots \rangle_\lambda$ is the canonical ensemble average at a particular value of λ parameter and $\partial H/\partial\lambda$ is the so-called driving-force. In this approach, an equilibrium simulation is performed for a set of λ-values in the interval between λ_i and λ_f, followed by numerical integration of the corresponding driving-force values.

As an alternative, intrinsically NE processes can be used to estimate the free-energy difference ΔF. In such a NE process, the coupling parameter $\lambda = \lambda(t)$ changes continuously throughout the simulation, and instead of an integration over equilibrium ensemble averages, Eq. (1), is replaced by an integration over instantaneous values of the driving-force,

$$W_{\rm dyn} = \int_0^{t_s} \frac{d\lambda}{dt} \frac{\partial H(\lambda)}{\partial \lambda}\bigg|_{\lambda(t)} dt, \tag{2}$$

where t_s is the switching time and $W_{\rm dyn}$ is the dynamical work done. Due to the irreversible nature of the process, dissipative entropy is produced, causing $W_{\rm dyn}$ to be a stochastic variable whose mean value, by the second law of thermodynamics, differs from $W_{\rm rev}$ by the relation

$$\Delta F = W_{\rm rev} = \overline{W_{\rm dyn}} - \overline{Q_{\rm diss}}, \tag{3}$$

where the overbar means an average over an ensemble of realizations of the NE process and $\overline{Q_{\rm diss}} \geqslant 0$ is the average dissipated heat. The latter is zero only in the quasistatic limit ($t_s \to \infty$). However, it can be shown [7] that the systematic error can be eliminated by combining the results of the processes realized in both directions (forward and backward) as long as the process is executed sufficiently slowly for linear-response theory to be valid. Accordingly, one has

$$\begin{aligned} \Delta F &\overset{=}{\equiv} \tfrac{1}{2}[W_{\rm rev}^{i\to f} - W_{\rm rev}^{f\to i}] \\ &\overset{=}{=} \tfrac{1}{2}\{[\overline{W_{\rm dyn}^{i\to f}} - \overline{Q_{\rm diss}^{i\to f}}] - [\overline{W_{\rm dyn}^{f\to i}} - \overline{Q_{\rm diss}^{f\to i}}]\} \\ &\overset{=}{=} \tfrac{1}{2}[\overline{W_{\rm dyn}^{i\to f}} - \overline{W_{\rm dyn}^{f\to i}}], \end{aligned} \tag{4}$$

where we have used the fact that $\overline{Q_{\rm diss}^{i\to f}} = \overline{Q_{\rm diss}^{f\to i}}$ under these conditions. Similarly, the systematic error can be estimated by

$$\overline{Q_{\rm diss}^{i\to f}} = \overline{Q_{\rm diss}^{f\to i}} = \frac{1}{2}[\overline{W_{\rm dyn}^{i\to f}} + \overline{W_{\rm dyn}^{f\to i}}]. \tag{5}$$

Eqs. (4) and (5) allow a systematic monitoring of the convergence of the results with the process rate, running a number of forward and backward realizations for a set of t_s values and plotting ΔF and the dissipation as a function of t_s.

While the comparison between the computational efficiencies of the equilibrium and NE methods is an active topic of investigation [35–38], it has been shown that the latter allows one to obtain accurate estimates of ΔF using only a few relatively short non-equilibrium simulations [7,8]. Indeed, due to the availability of straightforward error analysis and convergence protocols, the NE techniques serve as an attractive alternative to the standard equilibrium methodology.

In the following we present two specific thermodynamic paths $H(\lambda)$ that, respectively, are used to compute (i), the free-energy difference between Hamiltonians describing two different systems and, (ii) the temperature-dependence of the free energy for a given system Hamiltonian.

2.1. Free-energy difference between two systems: Hamiltonian interpolation method

Suppose we wish to compute the absolute free-energy of some system of interest described by a Hamiltonian $H_{\rm int}$ of the form

$$H_{\rm int} = K + U_{\rm int}(\{\mathbf{r}_i\}), \tag{6}$$

where K is the kinetic energy and $U_{\rm int}$ is the system of interest's interaction potential, which is a function of the set of particle coordinates and/or molecular degrees of freedom $\{\mathbf{r}_i\}$. Suppose further that there is a second system, in the same thermodynamic phase as that of the previous one, having a known free energy (analytical or numerical) and described by the Hamiltonian $H_{\rm ref}$, given by

$$H_{\rm ref} = K + U_{\rm ref}(\{\mathbf{r}_i\}), \tag{7}$$

with $U_{\rm ref}(\{\mathbf{r}_i\})$ its interaction potential.

The HI method consists of defining a parameterized Hamiltonian $H(\lambda)$ as a linear interpolation between the system of interest and reference Hamiltonians:

$$H(\lambda) = \lambda H_{\rm int} + (1-\lambda) H_{\rm ref}. \tag{8}$$

We define the forward process according to $\lambda_i = 1$ and $\lambda_f = 0$, transforming $H_{\rm int}$ into $H_{\rm ref}$.

The dynamical work for a given realization of the HI process is given by

$$W_{\rm dyn}^{i\to f} = \int_0^{t_s} \frac{d\lambda}{dt}(U_{\rm int} - U_{\rm ref})\,dt, \tag{9}$$

which, in practice, is estimated numerically.

Finally, combining the average results obtained from a number of independent realizations in the forward and backward switching processes, the desired free-energy is estimated as

$$F_{\rm int} = F(\lambda_i) = F_{\rm ref} + \frac{1}{2}[\overline{W_{\rm dyn}^{i\to f}} - \overline{W_{\rm dyn}^{f\to i}}]. \tag{10}$$

2.2. Free energy as a function of the temperature: Reversible Scaling method

Suppose the Helmholtz free energy $F_{\rm int}(T_0)$ of a system of interest is known at some temperature T_0 (e.g., computed using the method of previous section), and that we now wish to determine $F_{\rm int}(T)$ for other temperatures T. One way of doing this is repeating the free-energy calculation for each temperature of interest. Alternatively, this can be achieved using a single, constant-temperature MD simulation using the reversible-scaling (RS) technique [39,40]. The RS method is based on the parametric Hamiltonian

$$H_{\rm RS}(\lambda) = K + \lambda U_{\rm int}(\{\mathbf{r}_i\}), \tag{11}$$

where the potential energy is scaled by the coupling parameter λ. The configurational part of the classical partition function $Z_{\rm RS}(\lambda)$ of the RS Hamiltonian at temperature T_0 is given by

$$Z_{\rm RS}(\lambda) = \int d^{3N}\mathbf{r}\exp[-\lambda U(\{\mathbf{r}\})/k_B T_0] = Z_{\rm int}\left(T_0/\lambda\right), \tag{12}$$

which is equal to that of the partition function of the system of interest at temperature $T = T_0/\lambda$. In view of this relationship it can be shown [39] that the free energies of the scaled and physical systems are related according to

$$F_{\rm int}(T) = \frac{F_{\rm RS}(T_0;\lambda)}{\lambda} + \frac{f}{2}Nk_B T_0\frac{\ln\lambda}{\lambda}, \tag{13}$$

where N is the number of entities (i.e., atoms or molecules) in the system and f is the number degrees of freedom for each of them, e.g., $f = 3$ for atomic systems and $f = 6$ for a fluid composed of rigid molecules. Eq. (13), implies that each value of λ in the scaled Hamiltonian $H_{\rm RS}$ at a *fixed* temperature T_0 corresponds to the system of interest described by $H_{\rm int}$ at a temperature $T = T_0/\lambda$. In other words, the free energy of physical system as a function of temperature T can be obtained from $H(\lambda)$ by varying the scaling parameter λ at fixed temperature T_0. To this end the AS procedure can be applied, with $\lambda(t)$ varying from $\lambda(0) = 1$ to $\lambda(t_s) = \lambda_f$ to estimate the forward dynamical work along the isothermal scaling process,

$$W_{\rm dyn}^{1\to f} = \int_0^{t_s} \frac{d\lambda}{dt}U_{\rm int}\,dt. \tag{14}$$

Also carrying out the scaling process in the opposite direction and using Eq. (10), $F_{\rm int}(T)$ on the temperature interval between T_0 and T_0/λ_f is given by

$$F_{\rm int}(T) = \frac{F_{\rm int}(T_0)}{\lambda} + \frac{f}{2}Nk_B T_0\frac{\ln\lambda}{\lambda} + \frac{1}{2\lambda}[\overline{W_{\rm dyn}^{1\to\lambda}} - \overline{W_{\rm dyn}^{\lambda\to 1}}], \tag{15}$$

where λ varies between 1 and λ_f

It is important to note that the application of this approach requires knowledge of the absolute free energy of the system of interest at a temperature T_0, which can be computed using the HI method detailed in Section 2.1.

Finally, the RS method summarized above permits one to compute the *Helmholtz* free energy as a function of temperature for fixed volume. However, RS can also been generalized to compute the *Gibbs* free energy as a function of temperature for any desired pressure P [40]. In particular, for zero pressure, the scaling simulation detailed above, when applied under conditions of constant zero pressure $P = 0$ and temperature T_0, transfers directly to the temperature-dependence of the Gibbs free energy, replacing the Helmholtz free energy $F_{\rm int}$ by the Gibbs free energy $G_{\rm int}$ in Eq. (15), i.e.,

$$G_{\rm int}\left(P = 0,\ T\right) = \frac{G_{\rm int}(P = 0,\ T_0)}{\lambda} + \frac{f}{2}Nk_B T_0\frac{\ln\lambda}{\lambda} + \frac{1}{2\lambda}[\overline{W_{\rm dyn}^{1\to\lambda}} - \overline{W_{\rm dyn}^{\lambda\to 1}}]. \tag{16}$$

3. Uhlenbeck-Ford reference systems

In this section we describe the UF-based fluid-phase reference systems that we use to compute the absolute free energies of atomic and molecular fluids. In view of the particular applications that will be presented, we describe references for atomic fluids, as well as for rigid and flexible models for liquid water. All the reference systems are interacting fluids composed of atoms or molecules that repel each other according to the UF model, defined as [21–23]

$$U_{\rm UF}(\mathbf{r}) = -\frac{p}{\beta}\ln(1 - e^{-(r/\sigma)^2}), \tag{17}$$

where $\beta \equiv (k_B T)^{-1}$, σ is a length-scale parameter, r is an inter-particle distance and $p > 0$ is a scaling factor that controls the softness of the interactions. The UF model is a purely repulsive, smooth soft-sphere pairwise interaction that decays rapidly for increasing distances, diverges logarithmically at the origin, and is characterized by an energy scale controlled by the absolute temperature T.

The UF models feature a number of properties that render it a suitable choice to serve as a reference system for fluid-phase free-energy computations:

(i) The excess free energy of the UF fluid can be represented as a function of a single adimensional density parameter for any desired temperature,

$$F_{\rm UF}^{(\rm exc)}\left(x,\ T\right) = k_B T\sum_{n=1}^{\infty}\frac{\widetilde{B}_{n+1}(p)}{n}x^n, \tag{18}$$

where

$$x \equiv b\rho, \tag{19}$$

with ρ the system's number density, $b \equiv (\pi\sigma^2)^{3/2}/2$ and the $\widetilde{B}_{n+1}(p)$ are reduced virial coefficients that depend only on the scaling factor p and, in principle, can be computed exactly [22]. However, the effort associated with their calculation increases extremely rapidly with the order n such that only a limited number of them can actually be evaluated [22]. Nevertheless, a set of very accurate numerical representations of the free-energy functions in Eq. (18) is available for $p = 1, 25, 50, 75, 100$, and can be found in the Supplementary Material of Ref. [22].

(ii) There is only a single fluid phase, i.e., there is no liquid-gas transition, and this fluid phase is the only thermodynamically stable phase for $p \lesssim 100$ [23].

In the following we provide details concerning the UF-based reference systems and discuss how to apply them using the NE Hamiltonian-interpolation (NEHI) free-energy technique discussed in the previous Section.

3.1. Atomic models

As described previously [22], the application as a reference system

for the calculation of free energies of atomic fluids is straightforward. In this case, the thermodynamic path is defined as

$$H(\lambda) = \lambda U_{\text{int}} + (1-\lambda)U_{\text{UF}}, \tag{20}$$

transforming the interactions in the physical system into those of the UF model as λ varies from 1 to 0. Even when dealing with atomic fluids containing different species, such as in the case of liquid alloys, all particles interact according to the same UF model.

Determining the free-energy difference based on the forward and backward dynamical work estimators according to Eq. (4), the absolute Helmholtz free energy of the fluid of interest is given by

$$F_{\text{int}} = F_{\text{ig}} + F_{\text{UF}}^{(\text{exc})} + \frac{1}{2}[\overline{W_{\text{dyn}}^{1\to 0}} - \overline{W_{\text{dyn}}^{0\to 1}}], \tag{21}$$

where $F_{\text{UF}}^{(\text{exc})}$ is the known UF excess Helmholtz free energy and F_{ig} is the kinetic ideal gas contribution. In the case of a monoatomic system of N atoms with mass m, it is given by

$$F_{\text{ig}} = \frac{N}{\beta}\left[3\ln(\Lambda) + \ln(\rho) - 1 + \frac{1}{2N}\ln\left(2\pi N\right)\right], \tag{22}$$

where Λ is the de Broglie's thermal wavelength

$$\Lambda = \sqrt{\frac{\beta h^2}{2\pi m}}, \tag{23}$$

and last term on the right side is a logarithmic correction to Stirling's approximation.

For a binary mixture containing a total of N particles with concentrations X_A and X_B and masses m_A and m_B for species A and B, respectively, the ideal-gas part is given by

$$F_{\text{ig}} = \frac{N}{\beta}\Big\{X_A[3\ln(\Lambda_A) + \ln(\rho) - 1 + \ln(X_A)] + X_B[3\ln(\Lambda_B) + \ln(\rho) - 1 + \ln(X_B)] + \frac{1}{2N}\ln\left(2\pi N\right)\Big\}, \tag{24}$$

with Λ_A and Λ_B the de Broglie wavelengths associated with the masses m_A and m_B.

3.2. Rigid-body water models: UF/Rw

In the last 50 years, a plethora of empirical water models have been developed. A substantial fraction of these describe the water molecule as a rigid body in which the intramolecular degrees of freedom, such as OH bond length r_{eq} and HOH bond angle θ_{eq}, are fixed. Often, the interactions between the water molecules involve a LJ-type interaction between the oxygen atoms, supplied with Coulomb interactions between point charges located on a variety of positions, giving a potential of the form

$$U_{\text{int}} = \sum_{i,j>i}\left\{4\varepsilon\left[\left(\frac{\sigma}{r_{ij}}\right)^{12} - \left(\frac{\sigma}{r_{ij}}\right)^{6}\right] + \sum_{m,n}\frac{q_{im}q_{jn}}{r_{im,jn}}\right\} \tag{25}$$

where the indices i and j label molecules, m and n label the point charges within the molecules, r_{ij} is the distance between the oxygens of molecules i and j and the $r_{im,jn}$ are the distances between their respective charge centers m and n.

Because of the rigidity of the water molecules in these models, a natural choice for a reference system is one consisting of molecules with the same intramolecular structure. In addition, to decouple translational degrees of freedom from the rotational ones, it is convenient to design the interaction between molecules of the reference system to act on their respective centers of masses [18]. In this manner, the reference system we employ for rigid water models is characterized by the following elements:

- The reference system consists of rigid molecules that have the same geometry as that of the water model under consideration.
- The interaction between two molecules is given by the UF model, with the interparticle distance between them defined as the distance between their centers of masses.
- The reference molecules do not possess any charges.

The Hamiltonian of this reference system, which we will refer to as UF/Rw, is given by

$$H_{\text{UF/Rw}} = K_{\text{rot}}\left(\varphi_i, \mathbf{p}_{\varphi_i}\right) + K_{\text{trans}}\left(\{\mathbf{P}_i\}\right) + U_{UF}\left(\{\mathbf{R}_i\}\right), \tag{26}$$

where K_{rot} describes the rotational kinetic energy in terms of the molecules' Euler angles and associated canonical momenta, K_{trans} is the translational kinetic energy, which is a function of the total linear momenta $\{\mathbf{P}_i\}$ of the molecules of total mass M, and $U_{UF}(\{\mathbf{R}_i\})$ is the UF interaction between the molecular centers of mass $\{\mathbf{R}_i\}$.

The classical canonical partition function for a system of N such molecules can be written as

$$Z = \frac{1}{N!}Z_{\text{rot}}^N Z_{\text{trans}}^N, \tag{27}$$

where the rotational part is given by [41]

$$Z_{\text{rot}} = \sqrt{\frac{2\pi I_1 I_2 I_3}{\beta^3\hbar^6}}, \tag{28}$$

where I_1, I_2 and I_3 are the principal moments of inertia of the molecule, and the translational part is identical to that of an atomic system of N UF particles with mass M [22]. The corresponding absolute Helmholtz free energy of the UF/Rw system is then given by

$$F_{\text{UF/Rw}}(T) = -\frac{N}{\beta}\left[\frac{3}{2}\ln\left(\frac{2\pi M}{\beta h^2}\right) - \ln(\rho) + 1 - \frac{1}{2N}\ln\left(2\pi N\right) + \frac{1}{2}\ln\left(\frac{2\pi I_1 I_2 I_3}{\beta^3\hbar^6}\right)\right] + F_{\text{UF}}^{(\text{exc})}\left(x, T\right), \tag{29}$$

where x is the adimensional scaled density variable defined in Eq. (19). In this expression, the intermolecular contribution to the free energy is described entirely by $F_{\text{UF}}^{(\text{exc})}(x, T)$, with the other terms representing the translational and rotational ideal-gas contributions.

With the available numerical expressions for $F_{\text{UF}}^{(\text{exc})}(x, T)$, we use the thermodynamic path

$$H(\lambda) = \lambda H_{\text{int,rigid}} + (1-\lambda)H_{\text{UF/Rw}}, \tag{30}$$

connecting the fully-interacting rigid water model to the rigid UF/Rw reference. Then, performing forward and backward processes to estimate the work done along this thermodynamic path, the absolute Helmholtz free-energy of the fully-interacting water system is computed as

$$F_{\text{int,rigid}} = F_{\text{UF/Rw}} + \frac{1}{2}[\overline{W_{\text{dyn}}^{1\to 0}} - \overline{W_{\text{dyn}}^{0\to 1}}] \tag{31}$$

3.3. Flexible water models: UF/Fw

Another class of water models incorporates explicit flexibility into the molecule structure, allowing both stretching of the OH bonds as well as variation of the ∠HOH angle. To compute the free energy of fluids composed of such molecules we employ a flexible reference system in which the intermolecular interactions acting between the oxygen atoms are described by the UF model, whereas the intramolecular bond and angular dynamics are characterized by purely harmonic potentials. Specifically, the Hamiltonian of the flexible UF water (UF/Fw) model is given by

$$H_{\text{UF/Fw}} = K + U_{\text{intra}} + U_{\text{inter}} \tag{32}$$

where K is the sum of the kinetic energies of all atoms, U_{intra} is the sum of the intramolecular bond energies,

$$U_{\text{intra}} = \sum_{i=1}^{N} [U_{\text{OH}}(r_{i,1}) + U_{\text{OH}}(r_{i,2}) + U_{\text{HOH}}(\theta_i)], \tag{33}$$

in which $r_{i,1}$ and $r_{i,2}$ are the two OH bond lengths of molecule i and θ_i is its ∠HOH bond angle. The bond and angle potential energies are given by

$$U_{\text{OH}}(r) = \frac{1}{2}k_r(r - r_{\text{eq}})^2, \tag{34}$$

and

$$U_{\text{HOH}}(\theta) = \frac{1}{2}k_\theta(\theta - \theta_{\text{eq}})^2, \tag{35}$$

in which k_r and k_θ are the bond and angle spring constants, respectively, and r_{eq} and θ_{eq} are the corresponding equilibrium bond length and angle.

The intermolecular potential energy is given by

$$U_{\text{inter}} = \sum_{i>j} U_{\text{UF}}(r_{ij}), \tag{36}$$

with r_{ij} the distance between the oxygen atoms of molecules i and j.

Computing the canonical partition function (see the Supplementary Material for full details) one can show that the Helmholtz free energy of the flexible reference fluid is given by a sum of the UF free energy and a contribution due to the intramolecular interactions that can be expressed in analytical form,

$$F_{\text{UF/Fw}}(T) = -\frac{N}{\beta}\left[\frac{3}{2}\ln\left(\frac{8\pi^3 m_{\text{O}} m_{\text{H}}^2}{\beta^3 h^6}\right) - \ln\left(\frac{\rho}{8\pi^2}\right) + 1 - \frac{1}{2N}\ln(2\pi N) + 2\ln(I_r) + \ln(I_\theta)\right] + F_{\text{UF}}^{(\text{exc})}(x, T), \tag{37}$$

in which m_{O} and m_{H} are the masses of the oxygen atom and the proton, respectively, and where

$$I_r(k_r, \beta) = \frac{\sqrt{\frac{\pi}{2}}\left(\beta r_{\text{eq}}^2 k_r + 1\right)\left[\text{erf}\left(r_{\text{eq}}\sqrt{\frac{\beta k_r}{2}}\right) + 1\right]}{(\beta k_r)^{3/2}} + \frac{r_{\text{eq}}\exp\left(-\frac{1}{2}\beta r_{\text{eq}}^2 k_r\right)}{\beta k_r}, \tag{38}$$

and

$$I_\theta(k_\theta, \beta) = \sqrt{\frac{\pi}{2\beta k_\theta}}\exp\left(-\frac{1}{2\beta k_\theta}\right) \times Re\left[e^{i\theta_{\text{eq}}}\text{erfi}\left(\frac{1 - i\theta_{eq}\beta k_\theta}{\sqrt{2\beta k_\theta}}\right) - e^{i\theta_{\text{eq}}}\text{erfi}\left(\frac{1 + i(\pi - \theta_{eq})\beta k_\theta}{\sqrt{2\beta k_\theta}}\right)\right], \tag{39}$$

involve the imaginary error function erfi(z) [42]. These results are consistent with those reported recently [43]. As in Eq. (29), the intermolecular contribution to the free energy is described entirely by $F_{\text{UF}}^{(\text{exc})}(x, T)$, with the remaining terms representing the intramolecular vibrational and ideal-gas contributions.

With the availability of $F_{\text{UF/Fw}}$ we use the thermodynamic path

$$H(\lambda) = \lambda H_{\text{int,flexible}} + (1 - \lambda)H_{\text{UF/Fw}}, \tag{40}$$

connecting the flexible water model to the UF/Fw reference. Performing forward and backward processes, the absolute Helmholtz free-energy of the water system is calculated as

$$F_{\text{int,flexible}} = F_{\text{UF/Fw}} + \frac{1}{2}[\overline{W_{\text{dyn}}^{1\to 0}} - \overline{W_{\text{dyn}}^{0\to 1}}]. \tag{41}$$

4. Applications: results and discussion

In this section we describe how to implement and apply the described reference systems in the LAMMPS code to compute fluid free energies. Complete LAMMPS scripts, source code and auxiliary files are available [44].

As a first application, we determine the melting temperature of the hexagonal and cubic diamond phases of mW model. Next, we compute the free energies of the liquid Cu-Zr alloy as a function of composition. Finally, we apply the rigid and flexible molecular UF references to compute the Helmholtz free energies of the rigid TIP4P, SPC/E models as well as the flexible q-SPC/Fw potential.

4.1. Mono-atomic water (mW) model

To determine the melting temperature of the hexagonal and cubic-diamond structures of the mW model at zero pressure we compute the Gibbs free-energy curves $G(P, T)$ for the solid and liquid phases and find the temperature T_m at which they cross. To achieve this we follow Ref. [45], carrying out the following sequence of steps:

For the liquid:

(i) Perform an *NPT* MD simulation at zero pressure to determine the equilibrium density ρ_l of the liquid at a temperature $T_2 > T_m$.
(ii) Perform *NVT* MD simulations to compute the Helmholtz free energy F_l of the liquid at a density ρ_l and temperature T_2 using the AS procedure transforming the liquid of interest into the UF reference. For this case, $F_l(V_l, T_2) = G_l(P = 0, T_2)$.
(iii) Apply the RS method in the zero-pressure *NPT* ensemble to construct the Gibbs free energy curve $G_l(P = 0, T)$ of the liquid between T_1 and T_2.

For the solid:

(i) Perform a *NPT* MD simulation to determine the equilibrium density ρ_s of the crystalline solid at a temperature $T_1 < T_m$.
(ii) Perform *NVT* MD simulations to compute the Helmholtz free energy F_s of the crystalline solid at density ρ_s and temperature T_1. This is done applying the AS procedure connecting the interacting crystalline solid to an Einstein crystal. Since we consider the system under zero pressure, $F_s(\rho_s, T_1) = G_s(P = 0, T_1)$.
(iii) Apply the RS method under *NPT* ensemble at zero pressure $P = 0$ to construct the Gibbs free energy curve $G_s(P = 0, T)$ of the solid between T_1 and T_2.

For all phases we use computational cells containing 8, 000 mW atoms subject to periodic boundary conditions. Pressure and temperature control was obtained using a Parrinello-Rahman-type barostat [46] and a Langevin thermostat [47]. The corresponding equations of motion were integrated using velocity-Verlet algorithm with a time step of $\Delta t = 2$ fs.

For the liquid phase, step (i) entails determining the zero-pressure equilibrium volume at $T_2 = 290$ K. This is achieved using the following fix commands in the LAMMPS script:

```
fix f1 all nph iso 0.0 0.0 2.0
fix f2 all langevin 290 290 0.2 666
```

After an initial equilibration of 0.2 ns, we determine the average value of the volume over a time interval of 3.0 ns, giving an equilibrium number density of $\rho_l = 0.0334045(1)$ Å^{-3}, where the number in parentheses denotes the uncertainty in the final digit.

Next, in step (ii), we compute the Helmholtz free energy of liquid at this density, applying the NEHI procedure to compute the Helmholtz free-energy difference between the mW and UF fluids at $T = 290$ K and $\rho = \rho_l$. The switching process is implemented in the LAMMPS script by

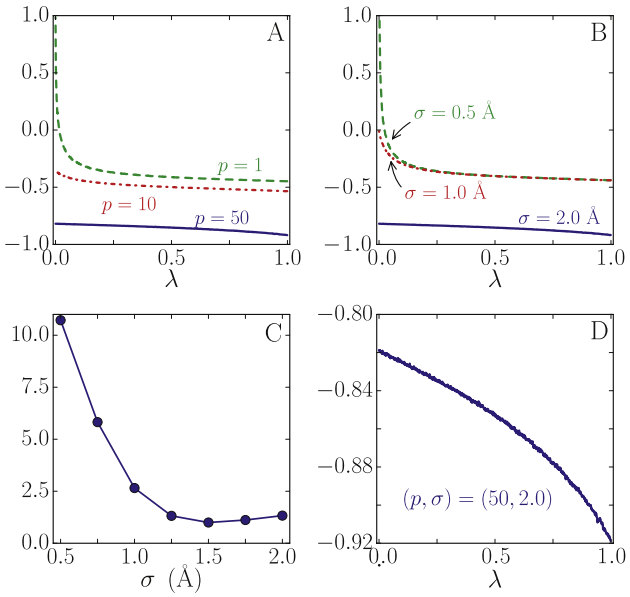

Fig. 1. Choice of parameters for UF reference to compute the free energy of the mW model. (A) Driving force $\partial H/\partial\lambda$ in units of eV per atom as a function of λ for various values p with $\sigma = 2.0$ Å. (B) Driving force $\partial H/\partial\lambda$ in units of eV per atom as a function of λ for various values of σ with $p = 50$. (C) Average dissipated heat $\overline{Q_{\text{diss}}}$ in units of meV per atom as a function of σ for $p = 50$. (D) Driving force as a function of λ for chosen parameter set $p = 50$ and $\sigma = 2.0$ Å.

invoking the `pair_style hybrid/overlay` command, followed by the `pair_coeff` instructions for the mW and UF models:

```
pair_style hybrid/overlay sw ufm 10.0
pair_coeff 1 1 sw mW.sw H2O
pair_coeff 1 1 ufm 1.2495 2.0
```

The value 10.0 in the `hybrid/overlay` command corresponds to a cut-off radius $r_c = 10$ Å. When involving the UF model, it should always be chosen such that $r_c = 5\sigma$, with σ the length scale parameter in the UF model. This requirement is due to the fact that the available excess free energies of the UF models [22] are given for this specific cut-off distance.

The parameter values of a reference system in the NEHI approach should be chosen such that the driving force $\partial H/\partial\lambda = U_{\text{int}} - U_{\text{ref}}$ is as smooth as possible to minimize the dissipated heat for a given switching rate. To this end it is useful to carry out a few short NEHI simulations to assess the behavior of the driving force and systematic error for different choices of the reference-system parameters. Fig. 1 shows the results of such an analysis obtained from simulations with $t_s = 10$ ps. In Fig. 1(a) we consider the value of the scaling parameter p during a single forward process from the mW liquid to the UF reference, monitoring the driving-force behavior for $p = 1$, 10 and 50 at $\sigma = 2.0$ Å. It can be seen that for small values of p the UF reference is too soft, allowing particles to become too close to each other and causing a near divergence [22] in the driving force close to $\lambda_f = 0$. Increasing p to 50 eliminates this problem, giving a slowly varying driving force over the entire λ-interval. Indeed, this choice for p has shown to be adequate for all NEHI calculations using the UF model, providing smooth driving-force curves characterized by small fluctuations. Similarly, if the length scale σ of the particle size is chosen too small, an analogous near-divergence issue occurs, as can be seen in Fig. 1(b). This can also be resolved by increasing its value. For this particular case a choice of $\sigma = 2.0$ Å gives a smooth slowly varying driving force. This choice can be further validated by measuring the mean dissipated heat $\overline{Q_{\text{diss}}}$ during the switching process as a function of σ, as displayed in Fig. 1(c). While Q_{diss} is large for smaller values, it decreases by an order of magnitude upon increasing σ, reaching a shallow minimum close to $\sigma = 1.5$ Å. The chosen parameter set with $p = 50$ and $\sigma = 2.0$ Å gives a slowly varying driving force with very small fluctuations, as can be seen in Fig. 1d).

In the corresponding `pair_coeff` command these values of p and σ are encoded in the first and second arguments after the `ufm` specification, respectively, with 1.2495 corresponding to the energy-scale $p\,k_B T = 1.2495$ eV, with $T = 290$ K.

In the `hybrid/overlay` pair style, the interactions between atoms are superpositions of two specified models and one can control the magnitude of each interaction type by changing the scale factor that multiplies the forces on the atoms using the fix `adapt` command. For example, to equilibrate a fluid in which the atoms interact only through the mW potential within the defined `hybrid/overlay` pair style given above, one can turn-off the UF interactions by scaling to zero the corresponding force contribution. This is accomplished by the commands.

```
variable lambda equal 0
fix f3 all adapt 0 pair ufm fscale 1 1 v_lambda
run 0
```

Here, `fscale` is a force scale factor defined in the employed pair styles. By default it is initialized at a value 1.0, but in the command sequence above it is set equal to the value of the variable `lambda`. Note that only the force contributions are scaled, whereas the potential-energy values are not. This is required since the driving force $\partial H/\partial\lambda$ always involves unscaled values of the potential energies. The purpose of the `run 0` command is to immediately update the forces according to this definition, without performing an MD time step.

The definitions above can be used to carry out the AS procedure linking the mW and UF fluids and compute the associated dynamical work value. In practice, this is accomplished by carrying out the following sequence of steps:

(1) First we set $\lambda = 1$ and equilibrate the system $H(\lambda = 1) = H_{\text{mW}}$ during a time interval of t_{eq}.
(2) We linearly change the λ parameter from $\lambda = 1$ to $\lambda = 0$ in a switching time t_s. This amounts to changing the particle interactions from mW at $t = 0$ to UF at $t = t_s$. We define this procedure to be the forward process.
(3) Next we set $\lambda = 0$ and equilibrate the system described by $H(\lambda = 0) = H_{\text{UF}}$ during a time of t_{eq}.
(4) We linearly change the λ parameter from $\lambda = 0$ to $\lambda = 1$ in a switching time t_s. This amounts to changing the particle interactions from UF at $t = 0$ to mW at $t = t_s$. We define this procedure to be the backward process.

Translating into `LAMMPS` script language, the forward process (steps 1–2) can be formulated as:

```
run t_eq
variable lambda1 equal ramp(1,0)
fix f4 all adapt 1 pair sw fscale 1 1 v_lambda1
variable lambda2 equal ramp(0,1)
fix f5 all adapt 1 pair ufm fscale 1 1 v_lambda2
run t_s
```

where `ramp(x,y)` is a function that linearly interpolates between the initial value `x` and the final value `y` during the simulation. The backward process (steps 3–4) is executed by repeating the same block of code, exchanging the values 1 and 0 in the `ramp` function.

We perform ten independent AS realizations (forward and backward) for the fluid system composed of 8000 atoms at $T_0 = 290$ K and the corresponding mW equilibrium density determined from the *NPT* simulations mentioned above. Before both switching processes the fluid system is equilibrated during $t_{\text{eq}} = 0.1$ ns. To verify the convergence of the free-energy in the AS processes, we execute simulations for different values of the switching time t_s. The results, depicted in Fig. 2, clearly show that the unbiased estimator, given by Eq. (10), converges very quickly. For instance, the relative difference between the results

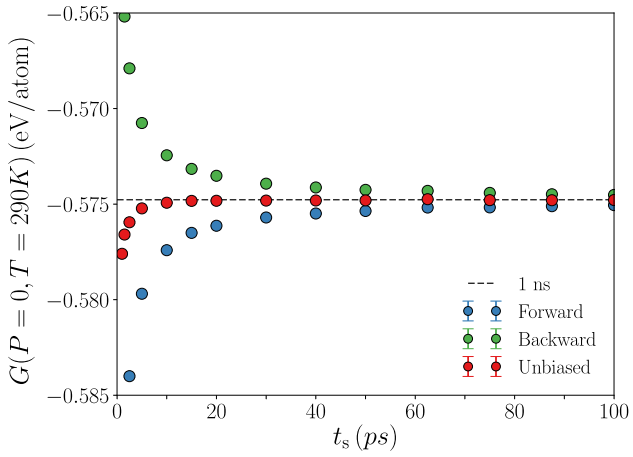

Fig. 2. Convergence of the absolute zero-pressure Gibbs free energy of the mW liquid at $T_0 = 290$ K obtained from NEHI simulations as function of the switching time t_s. Blue, green and red circles represent the results of forward, backward and the unbiased estimators, respectively. The error bars describing the statistical uncertainties are smaller than the symbol size for all cases. Dashed line represents unbiased estimator value for $t_s = 1.0$ ns. (For interpretation of the references to color in this figure legend, the reader is referred to the web version of this article.)

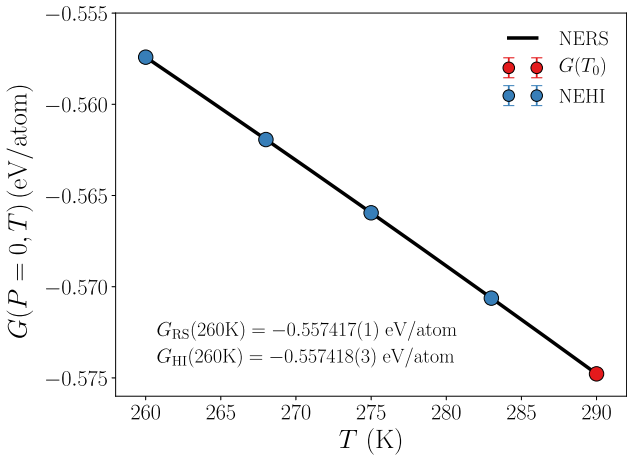

Fig. 3. Gibbs free-energy per atom of the mW liquid as a function of T at zero pressure. Black line depicts RS results. Red circle is the reference free-energy value $G(P = 0, T_0)$ used in Eq. (16). Blue circles represent free-energy values obtained using independent HI calculations. In all cases, the error bars are smaller than the symbol size. (For interpretation of the references to color in this figure legend, the reader is referred to the web version of this article.)

obtained for $t_s = 30$ ps and 1.0 ns (shown as the dashed line) is less than 10^{-4}.

Finally, in step (iii), we use the RS method to construct the zero-pressure Gibbs free-energy curve as a function of temperature for the mW liquid. As detailed earlier, these simulations are carried out at constant temperature and zero pressure. In the `LAMMPS` script this is accomplished by repeating the same combination of `fix nph` and `langevin` that is used to determine the equilibrium density of the fluid for the AS calculations. The RS path involves scaling of the Hamiltonian of interest by a factor of λ according to Eq. (11). Here, for the mW liquid, the RS simulations are carried out at $T_0 = 290$ K, for which the Gibbs free energy is known from the AS calculations described in the previous paragraph. The scaling parameter is varied between $\lambda = 1$ and $\lambda = \lambda_f = 290/260$, such that the covered temperature range is that between $T_0/\lambda = 290$ K and $T_0/\lambda_f = 260$ K. The temperature dependence of the Gibbs free energy is then computed using Eq. (16), where we use the reference value $G(T_0 = 290\text{ K}) = -0.574774(4)$ eV/atom obtained from the NEHI simulations with a switching time of $t_s = 1.0$ ns and determine the dynamical work values $W^{1\to\lambda}$ and $W^{\lambda\to 1}$ as the average over ten independent realizations of the RS process in forward and backward directions.

The implementation of the RS procedure is based on the same sequence of steps (1–4) used for the Hamiltonian interpolation simulations described above. The only difference is that the RS simulations require only a single `fix adapt` command to scale the Hamiltonian of interest. Before initiating the scaling, the mW liquid system is first equilibrated for $t_{eq} = 0.1$ ns. Next, the scaling parameter $\lambda(t)$ is varied linearly between 1 and λ_f during the switching time $t_s = 1.0$ ns. Fig. 3 shows the resulting zero-pressure Gibbs free energy of the mW liquid as a function of temperature. To verify the accuracy of the RS results, we have carried out a number of additional NEHI simulations (using $t_s = 1.0$ ns and 10 independent forward and backward realizations) to compute the Gibbs free energy in an independent manner at a number of temperatures in the interval between 260 and 290 K. The agreement between the results obtained in both methods is excellent. For instance, at $T = 260$ K, the relative error in the free-energy results is very small, $\sim 10^{-4}$%, and both methods are in agreement within these error bars.

Having computed the Gibbs free energy of the liquid phase, we now determine the zero-pressure absolute Gibbs free energies as a function of temperature of the hexagonal-diamond (*hd*) and cubic-diamond (*cd*) structures. This is accomplished using procedures that are essentially identical to those applied to the calculations for the liquid phase, using HI to compute the Gibbs free energy at a reference temperature of $T_0 = 260$ K, followed by RS simulations to determine its further temperature dependence. The main difference concerns the reference system in the HI calculations, which, for the crystalline phases, is chosen to be the Einstein crystal with a spring constant of 0.5 eV/Å^2. For both the HI and RS runs the systems were equilibrated during 0.2 ns prior to the switching runs, and the unbiased dynamical-work estimators were obtained from 10 independent forward and backward realizations using switching times of 0.4 and 0.8 ns, respectively. Full details are described in Ref. [8].

With the resulting RS free-energy curves for both crystalline phases we now determine their respective melting points by analyzing the free-energy differences $\Delta G(T) \equiv G_{\text{solid}}(T) - G_{\text{liquid}}(T)$ as a function of temperature. The results are shown in Fig. 4, which displays $\Delta G(T)$ for the

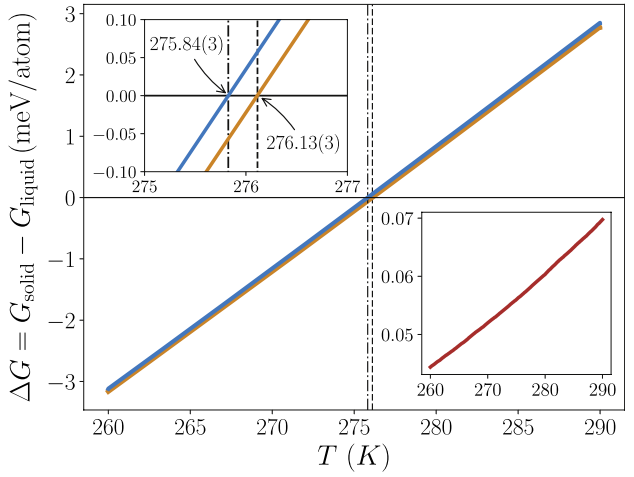

Fig. 4. Zero-pressure Gibbs free-energy difference between solid and liquid phases of mW model as a function of T. Orange and blue lines are RS curves for *hd* and *cd* structures, respectively. Vertical dashed lines describe the melting-temperature locations for both phases. Upper inset provides a zoom of melting point region. Red line in lower inset shows the free-energy difference $G_{cd}(T) - G_{hd}(T)$ between the *cd* and *hd* phases as a function of temperature. (For interpretation of the references to color in this figure legend, the reader is referred to the web version of this article.)

hexagonal and diamond cubic phases on the temperature interval between 260 and 290 K. A first observation is that, as expected, the *cd* phase is only metastable with respect to the *hd* structure, with the free-energy difference between them being positive across the entire temperature interval. Next, to determine the melting temperatures of both phases, we locate the temperature values T_m for which $\Delta G(T_m) = 0$. To this end we generate cubic-spline representations of the RS data for $\Delta G_{cd}(T)$ and $\Delta G_{hd}(T)$ and locate their respective roots, giving $T_m^{hd} = 276.13(3)$ K and $T_m^{cd} = 275.83(3)$ K, respectively. Here, the uncertainties in the final digit of the T_m values have been computed using the approach outlined in Ref. [45].

These results are consistent with the findings of Molinero and Moore [26], who reported the thermodynamic stability of the *hd* phase with respect to the *cd* structure. Our results for the melting-temperature values, however, are somewhat higher than those reported in Ref. [26], in particular for the *cd* phase: $T_m^{hd} = 275(1)$ K and $T_m^{cd} = 272(1)$ K. It is possible that these differences are related to the different methodologies used to determine the melting temperatures. The values reported in Ref. [26] were obtained using the coexistence method [48,49], and it has been shown [50] that this approach gives rise to melting temperatures that are systematically lower compared to those extracted from free-energy computations.

4.2. Cu-Zr liquid alloy

In the second application we apply the formalism to compute the free energy of a multicomponent fluid. In particular we consider the Cu-Zr liquid alloys systems, which have shown to be valuable in engineering applications due to their ability to produce bulk metallic glasses. We apply the nonequilibrium HI procedure to calculate the zero-pressure Gibbs free energy of Cu-Zr alloys as a function of composition at $T = 1800$ K, using the UF model as reference system.

All simulations were performed using computational cells containing 2000 atoms subject to periodic boundary conditions, with varying Cu and Zr fractions, X_{Cu} and X_{Zr}, respectively. The interparticle interactions are modeled by a second nearest-neighbor modified embedded atom method (MEAM-2NN) potential [29], with the adjustable parameters for Cu-Cu, Zr-Zr and Cu-Zr interactions taken from Refs. [31,51,52], respectively. The equations of motion are integrated using a time step of $\Delta t = 1$ fs.

As we are interested in determining the Gibbs free energy under zero pressure, we repeat the same procedure followed in Section 4.1, first performing equilibrium *NPT* MD simulations for a set of different Zr fractions to obtain the corresponding equilibrium number density, followed by *NVT* nonequilibrium HI calculations at the determined equilibrium density to compute the free-energy difference between the Cu-Zr liquid and the UF model. The HI procedure can be implemented in `LAMMPS` script following the same commands used for the mW model, with `fix adapt` scaling the respective intermolecular potentials. However, since we are dealing with more than one species, we must first define the reference interactions for all three types. Here, we choose all of them to be identical UF interactions, i.e., the reference UF models for the Cu-Cu, Zr-Zr and Cu-Zr interactions are specified by the same values of p, and σ. With this choice only the ideal gas part of the absolute reference free energy, Eq. (24), depends on the composition, whereas the interaction part does not. This can be encoded in the `fix adapt` command by introducing asterisks in its pair-type option:

```
fix f4 all adapt 1 pair meam/c fscale * * v_lambda1
fix f5 all adapt 1 pair ufm fscale * * v_lambda2
```

Using this approach we compute the free energy of the Cu-Zr liquid according to the unbiased estimator obtained from ten independent forward and backward realizations of the nonequilibrium HI process. We employ the parameter values $p = 50$ and $\sigma = 1.5$ Å for the UF reference. Before all HI realizations, the systems are first equilibrated for an interval $t_{\mathrm{eq}} = 0.1$ ns, followed by an HI process with a switching time $t_{\mathrm{s}} = 0.5$ ns.

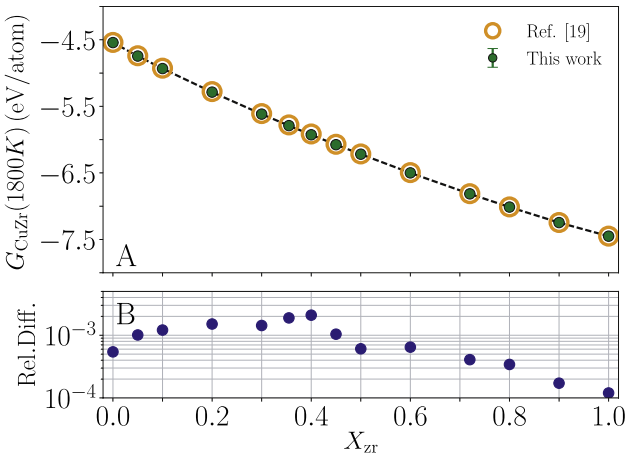

Fig. 5. Zero pressure Gibbs free energy as a function of Zr composition for the Cu-Zr liquid alloy at $T = 1800$ K. (A) Green circles depict present results, orange circles are data taken from Ref. [19]. The latter were computed using the equilibrium HI method with the LJ potential as a reference system. Dashed line serves as a guide to the eye. (B) Relative differences between present values and those of Ref. [19]. (For interpretation of the references to color in this figure legend, the reader is referred to the web version of this article.)

Table 1
Numerical values as a function of Zr composition. The columns contain, respectively, the atomic equilibrium number density ρ, the per-particle Gibbs free-energy difference ΔG between the MEAM and UF fluids, the absolute per-particle free-energy values for the UF model and the absolute zero-pressure Gibbs free energy per particle for the Cu-Zr liquid.

X_{Zr}	ρ atom/Å^3	$\Delta G/N$ eV/atom	G_{UF}/N eV/atom	G_{MEAM}/N eV/atom
1.000	0.03973	−6.28736(6)	−1.16271	−7.45007(6)
0.900	0.04221	−6.15403(2)	−1.09207	−7.24610(3)
0.800	0.04460	−6.01482(8)	−0.99818	−7.01300(8)
0.720	0.04665	−5.90906(9)	−0.90551	−6.81458(9)
0.600	0.05000	−5.76125(8)	−0.73821	−6.49947(8)
0.500	0.05306	−5.64985(9)	−0.57098	−6.22094(9)
0.450	0.05469	−5.59854(9)	−0.47768	−6.07622(9)
0.400	0.05635	−5.54842(2)	−0.37898	−5.92741(2)
0.355	0.05791	−5.50595(9)	−0.28401	−5.78996(9)
0.300	0.05987	−5.45625(3)	−0.16057	−5.61682(3)
0.200	0.06352	−5.36667(5)	0.08028	−5.28639(5)
0.100	0.06721	−5.27332(4)	0.34066	−4.93267(4)
0.050	0.06903	−5.22252(1)	0.47763	−4.74489(1)
0.000	0.07119	−5.19153(2)	0.64899	−4.54254(2)

The results are presented in Fig. 5 and Table 1. In the former, the present absolute free-energy values are compared to previously published data [19], which were obtained using equilibrium thermodynamic integration techniques using the LJ system as a reference system. Table 1 gives the corresponding numerical values. The agreement between the present calculations and the results reported in Ref. [19] is excellent, with relative discrepancies below ∼ 0.1 % for all compositions.

4.3. Rigid models: TIP4P and SPC/E

After the applications concerning atomic fluids we now turn to the case of molecular liquids, focusing in particular on liquid water. First, we consider two popular rigid-molecule descriptions, namely the SPC/E [33] and TIP4P [32] models, and compute their Helmholtz free energies as a function of temperature at a fixed density.

The adopted computational approach is similar to the 2-step

procedure employed to compute the temperature dependence of the free energy for the mW model. First, we compute the Helmholtz free energy at a reference temperature T_0 using the NEHI method, transforming the water-model interactions into those of the rigid UF water reference model, UF/Rw, described in Section 3.2. Next, we apply the NERS technique to extrapolate the free energy for temperatures beyond the reference value T_0.

For all calculations we use computational cells containing 4000 molecules at a density of 1.05 g/cm^3, subject to the usual periodic boundary conditions and the integration of the *NVT* MD equations of motion is carried out using a time step of $\Delta t = 2.0$ fs. The LJ parts for both rigid models are truncated, without shifting, at a cutoff distance of 8.5 Å and standard long-range corrections [24] are added to its energy. The long-range intermolecular electrostatic interactions are calculated using the particle-particle particle-mesh (PPPM) method [53] and intramolecular bond lengths and angles are held fixed using `SHAKE` [54] algorithm.

In `LAMMPS`, the SPC/E interactions with PPPM electrostatics are invoked by the generic `pair lj/cut/coul/long` and `kspace pppm` styles commands. For the TIP4P model, on the other hand, the model-specific `pair lj/cut/tip4p/long` and `kspace pppm/tip4p` styles are used. The UF/Rw reference interactions are activated by the `pair ufm/rw` command.

Although the implementation of the NEHI procedure for the water models into `LAMMPS` script is similar to that described in Section 4.1 for atomic fluids, additional care must be given to the PPPM force contributions. As the electrostatic interactions are switched off during the HI process, so must the long-range part evaluated using the PPPM method. This can be done using the same `fscale` variable introduced earlier in Section 4.1, invoking a `fix adapt` command in which the both the force contributions of the `pair` style as well as the long-range parts evaluated by the `kspace` command are scaled by the variable `lambda`:

```
fix f4 all adapt 1 pair lj/cut/coul/long fscale * * v_lambda &
kspace v_lambda fscale yes
```

For both rigid water models we compute the corresponding Helmholtz free-energy differences with respect to the UF/Rw system at $T = 225$ and 443 K, for which comparative free-energy information is available [4]. The values are computed using the unbiased estimator Eq. (10) obtained from 10 independent forward and backward NEHI realizations with a switching time of $t_s = 0.6$ ns. The parameters for the UF model are chosen to be $\sigma = 2.0$ Å and $p = 50$ for both cases. The corresponding absolute Helmholtz free-energy values for both rigid models are then computed using the absolute UF/Rw free energy given by Eq. (29), including the translational and rotational contributions to the ideal gas part. The resulting values for the absolute free-energy per molecule are given in Table 2 and they are in excellent agreement with those obtained by Vega et al. [4].

After the NEHI calculations for 225 and 443 K, we compute intermediate free-energy values form both models using the NEHI and NERS methods. For the former we consider the temperature $T = 250$, 300, 350 and 400 K and use the same simulation parameters as those used for 225 and 443 K. For the NERS computations we set $T_0 = 225$ K, obtaining the RS data from the unbiased estimator, Eq. (15), using 10 independent forward and backward simulations with $t_s = 1.0$ ns. The results, shown in Fig. 6, attest to the excellent agreement between both techniques.

Table 2
Helmholtz free-energy per molecule of liquid water as described by the SPC/E and TIP4P models at density $d = 1.05$ g/cm^3, obtained using the NEHI method. The values originally reported in Ref. [4] does not include the rotational contribution to the free energy and used a generic value of 1 Å for the thermal de Broglie wavelength. To allow a comparison with the present results, we have added the kinetic contribution to the data from Ref. [4] and adjusted the thermal wave-length value.

Model	T K	$\Delta F/N$ kcal/mol	$F_{UF}^{(exc)}/N$ kcal/mol	$F_{UF/Rw}/N$ kcal/mol	F_{liquid}/N kcal/mol	Ref. [4] kcal/mol
SPC/E	225	−25.7214(2)	17.9129	−5.2191	−13.0276(2)	−13.0298
SPC/E	443	−39.8195(4)	35.2684	−12.0651	−16.6162(4)	−16.6276
TIP4P	225	−16.4540(3)	9.6944	−5.1712	−11.9308(3)	−11.9307
TIP4P	443	−22.8003(4)	19.0872	−11.9707	−15.6838(4)	−15.6961

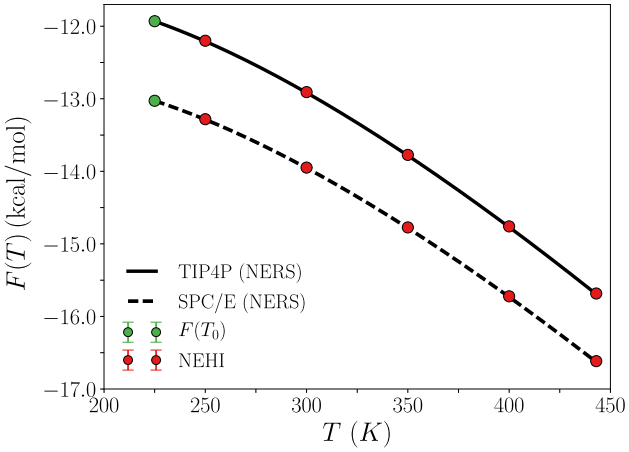

Fig. 6. Helmholtz free-energy per molecule as a function of temperature of TIP4P and SPC/E liquid water for a density of 1.05 g/cm^3. Circles represents results obtained using the NEHI approach. Error bars are smaller than symbol size. Full and dashed lines depict NERS results for the TIP4P and SPC/E models, respectively, using the green data points as reference values $F(T_0 = 225\ \text{K})$ in Eq. (15). (For interpretation of the references to color in this figure legend, the reader is referred to the web version of this article.)

4.4. Flexible model: q-SPC/Fw

Finally, we compute the free energy of the flexible q-SPC/Fw water model [34], using the flexible UF/Fw system as reference. The adopted simulation approach is the same as those used in the previous calculations, using the NEHI technique to compute the free-energy value at a specified temperature, followed by an NERS calculation to extrapolate its temperature dependence.

Compared to the calculations for the rigid water models the main difference is the computational cost. Due to the stiffness of the intramolecular harmonic interactions, the MD time step needs to be reduced substantially to preserve the numerical stability of the MD simulations. In particular, we use $\Delta t = 0.1$ fs, a factor 20 smaller than the value used for the rigid water molecules. Given the increased computational effort, we use a smaller simulation cell, containing 512 water molecules at a density of 1.0129 g/cm^3 subject to periodic boundary conditions.

We first compute the absolute Helmholtz free energy at $T = 255$ K applying the NEHI technique using the UF/Fw as the reference system, for which we set $p = 50$ and $\sigma = 1.8$ Å. The results are obtained from Eq. (41), using ten independent forward and backward realizations at a switching time of $t_s = 2.0$ ns. These results are shown in Table 3. Next, using the reference value at $T_0 = 255$ K, we extrapolate the temperature dependence up to $T = 270$ K using NERS with a switching time of $t_s = 1.0$ ns. The results are depicted in Fig. 7 and show excellent agreement between the NERS results and the NEHI data.

4.5. Efficiency of UF-based reference systems

The results presented in the previous sections attest to the applicability of UF-based models as reference systems in free-energy calculations for a variety of fluid-phase systems characterized by distinct

Table 3
Helmholtz free energy per molecule of the liquid q-SPC/Fw water model at density $d = 1.0129$ g/cm^3 for different temperatures as computed with the NEHI method using the UF/Rw system as reference.

T	$\Delta F/N$	$F_{\mathrm{UF}}^{(\mathrm{exc})}/N$	$F_{\mathrm{UF/Fw}}/N$	F_{liquid}/N
K	kcal/mol	kcal/mol	kcal/mol	kcal/mol
255	−13.531(1)	6.061	−2.365	−9.835(1)
260	−13.556(2)	6.180	−2.472	−9.848(2)
265	−13.582(2)	6.298	−2.580	−9.864(2)
270	−13.610(2)	6.417	−2.688	−9.881(2)

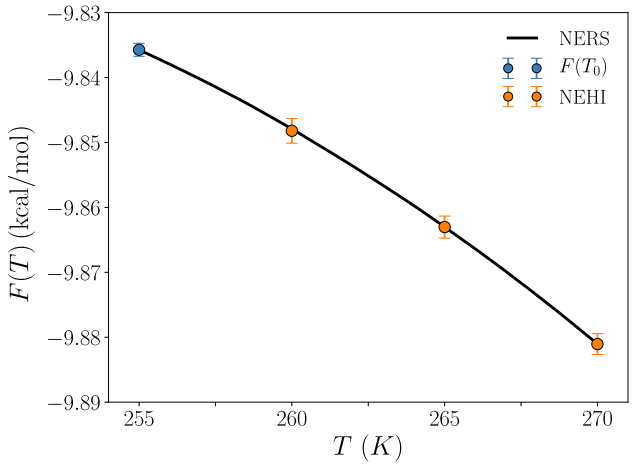

Fig. 7. Helmholtz free-energy per molecule as a function of temperature for q-SPC/Fw (full line) liquid water at a density of 1.0129 g/cm^3. Circles represent value computed using the NEHI technique. Solid line represents NERS results obtained using the reference free-energy value $F(T_0 = 255\ \mathrm{K})$ indicated by the green circle. (For interpretation of the references to color in this figure legend, the reader is referred to the web version of this article.)

interaction types.

Not only do they allow free-energy values to be computed with high-precision, they also do so in a computationally efficient manner. The rapid convergence of the unbiased estimator in Fig. 2 is illustrative for this, with trajectories as short as only 30 ps giving results that are essentially indistinguishable from those obtained from simulations covering a time interval of 1.0 ns.

Quick convergence is a consequence of small dissipation along the switching simulations, characterizing a smooth, close-to-equilibrium process. For a given system of interest, the rate of dissipation in NEHI calculations is largely determined by the choice of reference system. While the above results indicate that the UF-based models are a competitive option, it is not clear whether or not they are superior to other common choices. To shed light on this issue we carry out a comparison with one of the most-frequently employed reference systems in fluid-phase free-energy calculations, namely those based on the LJ model.

For this purpose, we carry out additional NEHI simulations for the atomic $Cu_{50}Zr_{50}$ liquid alloy and molecular TIP4P fluid, respectively, using UF and LJ-based reference systems for both. In particular, as a quantitative measure of efficiency, we compute the ratio of the average dissipated heat $\overline{Q_{\mathrm{diss}}}$ and the unbiased estimator for the free-energy difference ΔF as a function of the switching time t_s. The values for $\overline{Q_{\mathrm{diss}}}$ and ΔF were computed using Eqs. (4) and (5), employing the results of ten independent forward and backward processes. The UF-model parameters are the same as those used in the previous sections. For the liquid alloy, the chosen parameters of the LJ reference coincide with those used in Ref. [19]. For the TIP4P liquid, the LJ parameters are the same as those in the proper model definition.

The resulting ratios are depicted in Fig. 8. They decay with increasing switching time according to $\sim 1/t_s$, which is expected for

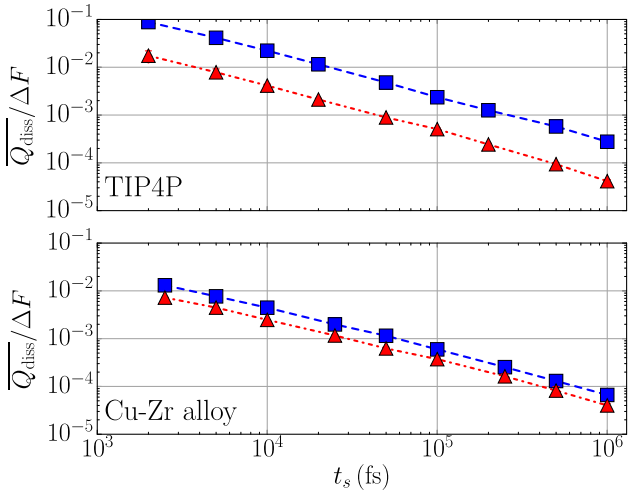

Fig. 8. Average ratios of dissipated heat and free-energy difference as a function of t_s in NEHI simulations using the UF (triangles) and LJ (squares) models as reference systems. Results are shown for the TIP4P water model and the $Cu_{50}Zr_{50}$ liquid alloy as described by the MEAM-2NN potential. Dashed lines serve as guides to the eye.

nonequilibrium processes in the linear regime [7]. In addition, the UF-based references display superior efficiency for both cases, giving a substantially smaller dissipation for given switching time. Indeed, for the TIP4P case, the ratio obtained using the UF reference system is almost an order of magnitude smaller compared to the results for the LJ reference. These results clearly show that the UF model provides a general and efficient reference system for the calculation of fluid-phase free energies of systems characterized by different interactions.

5. Summary

In this paper we provide a guide for computing free energies of fluid-phase systems using nonequilibrium techniques within the `LAMMPS` MD simulation package. In addition to describing `LAMMPS` implementation details and making available the computational tools in the form of full source code, scripts and auxiliary files [44], we discuss in detail the purely repulsive, ultrasoft UF pair potential as a reference system. Not only is the UF model useful for atomic fluids, either monoatomic or mixtures, it can also be used to construct reference systems for molecular fluids.

This is illustrated in a number of application in which free energies of fluids characterized by fundamentally different interaction types are computed. In particular, we consider atomic mW model for water, a binary liquid alloy described by an MEAM-2NN potential and three molecular models for water, two of them rigid and one flexible. In all applications, the corresponding UF-based reference systems provide smooth thermodynamic paths that allow accurate and efficient free-energy calculations. In particular, comparing the results to the LJ model, which has been frequently been used as a reference system for fluids, the UF is much smoother in that it leads to substantially lower dissipation in a given switching processes.

The techniques described in this paper, together with the supplied source code, scripts and post-processing files, provide a platform on which fluid-phase free energies can be easily and efficiently computed using the `LAMMPS` code. In addition to being useful for the development of new models for liquid phases, the tools may also find applications in the construction of community databases containing thermodynamic properties of existing models.

6. Data availability

The raw/processed data required to reproduce these findings cannot

be shared at this time due to technical or time limitations.

CRediT authorship contribution statement

Rodolfo Paula Leite: Software, Validation, Formal analysis, Investigation, Data curation, Writing - original draft, Visualization. **Maurice de Koning:** Conceptualization, Methodology, Writing - review & editing, Supervision.

Acknowledgments

We acknowledge support from FAPESP Grants No. 2013/08293-7 and 2016/23891-6, CNPq. This study was financed in part by the Coordenação de Aperfeiçoamento de Pessoal de Nível Superior – Brasil (CAPES) – Finance Code 001. The authors acknowledge the National Laboratory for Scientific Computing (LNCC/MCTI, Brazil) for providing HPC resources of the SDumont supercomputer, URL: http://sdumont.lncc.br.

Appendix A. Supplementary material

The Supplementary material describes the details of the calculation of the classical partition function and the corresponding Helmholtz free energy for the UF/Fw model. Supplementary data associated with this article can be found, in the online version, at https://doi.org/10.1016/j.commatsci.2018.12.029.

References

[1] D.A. Kofke, Fluid Phase Equilib. 228–229 (2005) 41–48.
[2] J.G. Kirkwood, J. Chem. Phys. 3 (5) (1935) 300–313.
[3] D. Frenkel, B. Smit, Understanding Molecular Simulation, Academic Press, San Diego, 2002.
[4] C. Vega, E. Sanz, J.L.F. Abascal, E.G. Noya, J. Phys.: Condens. Matter 20 (15) (2008) 153101.
[5] L. Li, T. Totton, D. Frenkel, J. Chem. Phys. 146 (21) (2017) 214110.
[6] M. Watanabe, W.P. Reinhardt, Phys. Rev. Lett. 65 (26) (1990) 3301–3304.
[7] M. de Koning, J. Chem. Phys. 122 (10) (2005) 104106.
[8] R. Freitas, M. Asta, M. de Koning, Comput. Mater. Sci. 112 (Part A) (2016) 333–341.
[9] C. Jarzynski, Phys. Rev. Lett. 78 (14) (1997) 2690–2693.
[10] C. Jarzynski, Phys. Rev. E 56 (5) (1997) 5018–5035.
[11] C. Jarzynski, Annu. Rev. Condens. Matter Phys. 2 (1) (2011) 329–351.
[12] D. Frenkel, A.J.C. Ladd, J. Chem. Phys. 81 (7) (1984) 3188–3193.
[13] M. de Koning, A. Antonelli, Phys. Rev. E 53 (1) (1996) 465.
[14] C. Vega, E.G. Noya, J. Chem. Phys. 127 (15) (2007) 154113.
[15] M.C. Abramo, C. Caccamo, D. Costa, P.V. Giaquinta, G. Malescio, G. Muna, S. Prestipino, J. Chem. Phys. 142 (21) (2015) 214502.
[16] J.Q. Broughton, G.H. Gilmer, J. Chem. Phys. 79 (10) (1983) 5095–5104.
[17] J.Q. Broughton, X.P. Li, Phys. Rev. B 35 (1987) 9120–9127.
[18] S. Habershon, D.E. Manolopoulos, Phys. Chem. Chem. Phys. 13 (2011) 19714–19727.
[19] J.-P. Harvey, A.E. Gheribi, P. Chartrand, J. Chem. Phys. 135 (8) (2011) 084502.
[20] J.K. Johnson, J.A. Zollweg, K.E. Gubbins, Mol. Phys. 78 (3) (1993) 591–618.
[21] G. Uhlenbeck, G. Ford, Studies in Statistical Mechanics – The Theory of Linear Graphs with Application to the Theory of the Virial Development of the Properties of Gases vol. 2, North-Holland, 1962.
[22] R. Paula Leite, R. Freitas, R. Azevedo, M. de Koning, J. Chem. Phys. 145 (19) (2016) 194101.
[23] R. Paula Leite, P.A. Santos-Flórez, M. de Koning, Phys. Rev. E 96 (2017) 032115.
[24] M.P. Allen, D.J. Tildesley, D.J. Tildesley, Computer Simulation of Liquids, Oxford University Press, 2017.
[25] S. Plimpton, J. Comput. Phys. 117 (1) (1995) 1–19.
[26] V. Molinero, E.B. Moore, J. Phys. Chem. B 113 (13) (2009) 4008–4016.
[27] M.I. Baskes, Phys. Rev. B 46 (1992) 2727–2742.
[28] M. Baskes, Mater. Sci. Eng. A 261 (1) (1999) 165–168.
[29] B.-J. Lee, M.I. Baskes, Phys. Rev. B 62 (2000) 8564–8567.
[30] B.-J. Lee, M. Baskes, H. Kim, Y. Koo Cho, Phys. Rev. B 64 (2001) 184102.
[31] B.-J. Lee, J.-H. Shim, M.I. Baskes, Phys. Rev. B 68 (2003) 144112.
[32] W.L. Jorgensen, J. Chandrasekhar, J.D. Madura, R.W. Impey, M.L. Klein, J. Chem. Phys. 79 (2) (1983) 926–935.
[33] H.J.C. Berendsen, J.R. Grigera, T.P. Straatsma, J. Phys. Chem. 91 (24) (1987) 6269–6271.
[34] F. Paesani, W. Zhang, D.A. Case, T.E. Cheatham, G.A. Voth, J. Chem. Phys. 125 (18) (2006) 184507.
[35] G. Hummer, J. Chem. Phys. 114 (17) (2001) 7330–7337.
[36] H. Oberhofer, C. Dellago, P.L. Geissler, J. Phys. Chem. B 109 (14) (2005) 6902–6915.
[37] X. Daura, R. Affentranger, A.E. Mark, ChemPhysChem 11 (17) (2010) 3734–3743.
[38] C. Dellago, G. Hummer, Entropy 16 (1) (2014) 41–61.
[39] M. de Koning, A. Antonelli, S. Yip, Phys. Rev. Lett. 83 (1999) 3973–3977.
[40] M. de Koning, A. Antonelli, S. Yip, J. Chem. Phys. 115 (24) (2001) 11025–11035.
[41] G. Herzberg, Molecular Spectra and Molecular Structure: Spectra of diatomic molecules, Van Nostrand, 1945.
[42] J. Powers, M. Sen, Mathematical Methods in Engineering, Cambridge University Press, 2015.
[43] A. Farhi, B. Singh, New J. Phys. 18 (2) (2016) 023039.
[44] For full source code, scripts and auxiliary files, see. < http://github.com/plrodolfo/FluidFreeEnergyforLAMMPS > .
[45] S. Ryu, W. Cai, Modell. Simul. Mater. Sci. Eng. 16 (8) (2008) 085005.
[46] W. Shinoda, M. Shiga, M. Mikami, Phys. Rev. B 69 (13) (2004) 134103.
[47] T. Schneider, E. Stoll, Phys. Rev. B 17 (1978) 1302–1322.
[48] J.R. Morris, C.Z. Wang, K.M. Ho, C.T. Chan, Phys. Rev. B 49 (5) (1994) 3109–3115.
[49] J.R. Morris, X. Song, J. Chem. Phys. 116 (21) (2002) 9352–9358.
[50] R. García Fernández, J.L.F. Abascal, C. Vega, J. Chem. Phys. 124 (14) (2006) 144506.
[51] Y.-M. Kim, B.-J. Lee, M.I. Baskes, Phys. Rev. B 74 (2006) 014101.
[52] Y.-M. Kim, B.-J. Lee, J. Mater. Res. 23 (4) (2008) 1095–1104.
[53] R.W. Hockney, Computer Simulation Using Particles, Taylor & Francis Group, 2017.
[54] J.-P. Ryckaert, G. Ciccotti, H.J. Berendsen, J. Comput. Phys. 23 (3) (1977) 327–341.